Inorganic Chemistry

Article

Ni$_3$(Mo$_2$O$_8$)(XO$_3$) (X = Se, Te): The First Nickel Selenite- and Tellurite-Containing Mo$_4$ Clusters

Hai-Long Jiang,[†,‡] Zhi Xie,[†,‡] and Jiang-Gao Mao*,[†]

State Key Laboratory of Structural Chemistry, Fujian Institute of Research on the Structure of Matter, Chinese Academy of Sciences, Fuzhou 350002, P. R. China, and Graduate School of the Chinese Academy of Sciences, Beijing 100039, P. R. China

Two new nickel(II) molybdenum(VI) selenium(IV) and tellurium(IV) oxides generally formulated as Ni$_3$(Mo$_2$O$_8$)(XO$_3$) (X = Se, Te) have been synthesized by solid-state reactions of NiO, MoO$_3$, and SeO$_2$ (or TeO$_2$). Both compounds feature 3D network structures built of [Mo$_4$O$_{16}$]$^{8-}$ tetranuclear cluster units and 2D nickel(II) selenite or tellurite layers. The nickel(II) selenite layer in Ni$_3$(Mo$_2$O$_8$)(SeO$_3$) is formed by [Ni$_6$O$_{22}$]$^{32-}$ hexanuclear clusters interconnected by selenite groups whereas the thick nickel(II) tellurite layer in Ni$_3$(Mo$_2$O$_8$)(TeO$_3$) is constructed by corrugated nickel(II) oxide chains bridged by the tellurite groups. The results of magnetic property measurements indicate that there are considerable ferromagnetic interactions between nickel(II) centers in both compounds. Their optical properties and band structures have been also studied.

Introduction

Metal selenites or tellurites can adopt many unusual structures due to the presence of the stereochemically active lone-pair electrons.[1] The asymmetric coordination polyhedron adopted by the Se^{IV} or Te^{IV} atom may result in noncentrosymmetric structures with consequent interesting physical properties, such as nonlinear optical second-harmonic generation (SHG).[2–5] Transition-metal ions with d^0 electronic configuration such as Ti^{4+}, Nb^{5+}, Mo^{6+}, W^{6+}, etc, which are susceptible to second-order Jahn−Teller distortions, have been introduced into the metal selenite or tellurite systems to enhance the SHG properties.[3–5] Recent studies also indicate that the activation of both selenite or tellurite anions and molybdate (or tungstate) for lanthanide ions can also afford new luminescent materials in the near-IR region.[6] We deem that the combination of the lone-pair electrons of Se^{IV} or Te^{IV} with the distorted MoO$_6$ octahedron may lead to new compounds in Ni−Mo^{VI}−Se^{IV}/Te^{IV}−O systems with novel structures and unusual physical properties, such as magnetic or optical properties. So far, only a Ni−Mo^{VI}−Te^{VI}−O phase, [Ni(H$_2$O)$_6$]$_3$[TeMo$_6$O$_{24}$], has been reported,[7] and no nickel molybdenum(VI) selenite or tellurite has been structurally characterized. Our exploration of new phases in nickel molybdenum(VI) selenite or tellurite systems led to two novel compounds, namely, Ni$_3$(Mo$_2$O$_8$)(XO$_3$) (X = Se, Te). Despite their similar chemical formulas, they display two different types of 3D structures containing [Mo$_4$O$_{16}$]$^{8-}$ tetranuclear cluster units and [Ni$_6$O$_{22}$]$^{32-}$ hexanuclear clusters or 1D nickel oxide chains. Herein, we report their syntheses, band and crystal structures, and magnetic properties.

* To whom correspondence should be addressed. E-mail: mjg@fjirsm.ac.cn.

† Fujian Institute of Research on the Structure of Matter, Chinese Academy of Sciences.

‡ Graduate School of the Chinese Academy of Sciences.

(1) (a) Wickleder, M. S. *Chem. Rev.* **2002**, *102*, 2011 and references therein. (b) Verma, V. P. *Thermochim. Acta* **1999**, *327*, 63 and references therein.

(2) Kong, F.; Huang, S.-P.; Sun, Z.-M.; Mao, J.-G.; Cheng, W.-D. *J. Am. Chem. Soc.* **2006**, *128*, 7750.

(3) (a) Hart, R. T.; Ok, K.-M.; Halasyamani, P. S.; Zwanziger, J. W. *Appl. Phys. Lett.* **2004**, *85*, 938. (b) Porter, Y.; Halasyamani, P. S. *J. Solid State Chem.* **2003**, *174*, 441. (c) Goodey, J.; Broussard, J.; Halasyamani, P. S. *Chem. Mater.* **2002**, *14*, 3174. (d) Ok, K.-M.; Halasyamani, P. S. *Chem. Mater.* **2001**, *13*, 4278.

(4) (a) Ra, H.-S.; Ok, K.-M.; Halasyamani, P. S. *J. Am. Chem. Soc.* **2003**, *125*, 7764. (b) Ok, K.-M.; Halasyamani, P. S. *Inorg. Chem.* **2004**, *43*, 4248. (c) Ok, K.-M.; Orzechowski, J.; Halasyamani, P. S. *Inorg. Chem.* **2004**, *43*, 964. (d) Goodey, J.; Ok, K.-M.; Broussard, J.; Hofmann, C.; Escobedo, F. V.; Halasyamani, P. S. *J. Solid State Chem.* **2003**, *175*, 3.

(5) (a) Harrison, W. T. A.; Dussack, L. L.; Jacobson, A. J. *J. Solid State Chem.* **1996**, *125*, 234. (b) Johnston, M. G.; Harrison, W. T. A. *Inorg. Chem.* **2001**, *40*, 6518. (c) Balraj, V.; Vidyasagar, K. *Inorg. Chem.* **1999**, *38*, 5809. (d) Balraj, V.; Vidyasagar, K. *Inorg. Chem.* **1999**, *38*, 3458.

(6) Shen, Y. L.; Jiang, H. L.; Xu, J.; Mao, J. G.; Cheah, K. W. *Inorg. Chem.* **2005**, *44*, 9314.

(7) Lorenzo-Luis, P. A.; Martin-Zarza, P.; Gili, P.; Saez-Puche, R.; Jimenez-Jimenez, J.; Rodriguez-Castellon, E.; Ruiz-Perez, C.; Gonzalez-Platas, J.; Solans, X. *Eur. J. Solid State Inorg. Chem.* **1997**, *34*, 1259.

Experimental Section

Materials and Instrumentation. All of the chemicals except NiO were analytically pure from commercial sources and used without further purification. Neodymium(III) oxide, transition-metal oxides, and halides were purchased from the Shanghai Reagent Factory, and TeO$_2$ (99+%) and SeO$_2$ (99+%) were purchased from Acros Organics. NiO was synthesized by heating Ni$_2$O$_3$ in air at 610 °C for 12 h, and its purity was checked by X-ray powder diffraction (XRD) (see the Supporting Information).[8a] XRD patterns were collected on a XPERT-MPD $\theta-2\theta$ diffractometer. The chemical compositions of the two compounds were analyzed by a field-emission scanning-electron microscope (FESEM, JSM6700F) equipped with an energy dispersive X-ray spectroscope (EDS, Oxford INCA). The absorption spectra were recorded on a PE Lambda 900 UV−vis spectrophotometer in the wavelength range of 200−2200 nm. The absorption spectra were determined by the diffuse-reflectance technique.[8b] $F(R)$ and R are linked by $F(R) = (1 - R)^2/2R$, where R is the reflectance and $F(R)$ is the Kubelka−Munk remission function. The minima in the second-derivative curves of the Kubelka−Munk function are taken as the position of the absorption bands. IR spectra were recorded on a Magna 750 FT-IR spectrometer as KBr pellets in the range of 4000−400 cm^{-1}. Thermogravimetric analyses (TGA) were carried out with a NETZSCH STA 449C unit, at a heating rate of 10 °C/min under a static air atmosphere. Magnetic susceptibility measurements on polycrystalline samples were performed with a PPMS-9T magnetometer in the temperature range 2−300 K.

Preparation of Ni$_3$(Mo$_2$O$_8$)(SeO$_3$). Green brick-shaped crystals of Ni$_3$(Mo$_2$O$_8$)(SeO$_3$) were initially prepared by the solid-state reaction of a mixture of Nd$_2$O$_3$ (0.118 g, 0.35 mmol), MoO$_3$ (0.050 g, 0.35 mmol), NiCl$_2$ (0.045 g, 0.35 mmol), and SeO$_2$ (0.155 g, 1.4 mmol) in our attempt to prepare a Nd−Mo−Ni−Se−O−Cl phase. The reaction mixture was thoroughly ground and pressed into a pellet, which was then sealed into an evacuated quartz tube. The quartz tube was heated at 300 °C for 1 day and at 700 °C for 5 days, then slowly cooled to 295 °C at 4.5 °C/hr. It was finally cooled to room temperature in 16 h. Results of the EDS elemental analyses gave a molar ratio of Ni/Mo/Se equal to 3.2/1.9/1.0, which is in good agreement with the one determined from single-crystal X-ray structural analysis. Though Nd(III) is not present in Ni$_3$(Mo$_2$O$_8$)(SeO$_3$), the addition of Nd$_2$O$_3$ helps the crystallization of Ni$_3$(Mo$_2$O$_8$)(SeO$_3$), and the quality of the crystals is very poor when the synthesis is carried out in the absence of Nd$_2$O$_3$. The pure powder product of Ni$_3$(Mo$_2$O$_8$)(SeO$_3$) was obtained quantitatively by the reaction of a mixture of NiO/MoO$_3$/SeO$_2$ in a molar ratio of 3:2:1 at 710 °C for 6 days in a similar procedure described above (see the Supporting Information). IR data (KBr, cm^{-1}): 961 (vs), 928 (vs), 858 (s), 764 (m), 710 (m), 656 (s), 624 (s), 524 (m), 462 (m), 442 (w), 410 (w).

Preparation of Ni$_3$(Mo$_2$O$_8$)(TeO$_3$). Green brick-shaped crystals of Ni$_3$(Mo$_2$O$_8$)(TeO$_3$) were prepared by the solid-state reaction of a mixture containing NiO (37.3 mg, 0.5 mmol), MoO$_3$ (72.0 mg, 0.5 mmol), and TeO$_2$ (239.4 g, 1.5 mmol). The reaction mixture was thoroughly ground and pressed into a pellet, which was then sealed into an evacuated quartz tube. The quartz tube was heated at 720 °C for 6 days and then cooled to 270 °C at 4.5 °C/hr before switching off the furnace. The EDS elemental analyses gave a molar ratio of Ni/Mo/Te equal to 3.1/2.2/1.0, which is in good agreement with the one determined from single-crystal X-ray structural analysis. After proper structural analysis, a pure sample of

(8) (a) Barrett, C. A.; Evans, E. B. *J. Am. Ceram. Soc.* **1964**, *47*, 533. (b) Kubelka, P.; Munk, F. *Z. Tech. Phys.* **1931**, *12*, 593.

Table 1. Crystal Data and Structural Refinements for Ni$_3$(Mo$_2$O$_8$)(XO$_3$) (X = Se, Te)

	Ni$_3$(Mo$_2$O$_8$)(SeO$_3$)	Ni$_3$(Mo$_2$O$_8$)(TeO$_3$)
fw	622.97	671.61
space group	$P\bar{1}$ (No. 2)	$C2/m$ (No. 12)
a, Å	6.4630(7)	9.562(3)
b, Å	6.4654(4)	8.756(3)
c, Å	10.0262(5)	10.082(3)
α, deg	73.949(10)	90
β, deg	86.288(17)	103.228(7)
γ, deg	84.856(16)	90
V, Å^3	400.65(5)	821.7(4)
Z	2	4
D_{calcd}, g·cm^{-3}	5.164	5.429
μ, mm^{-1}	14.565	13.254
GOF on F^2	0.984	1.106
R1, wR2 $[I>2\sigma(I)]^a$	0.0357, 0.0847	0.0175, 0.0413
R1, wR2 (all data)	0.0412, 0.0878	0.0186, 0.0418

^{a} R1 = $\sum ||F_o| - |F_c||/\sum |F_o|$, wR2 = $\{\sum w[(F_o)^2 - (F_c)^2]^2/\sum w[(F_o)^2]^2\}^{1/2}$.

Ni$_3$(Mo$_2$O$_8$)(TeO$_3$) was obtained quantitatively by the reaction of a mixture of NiO/MoO$_3$/TeO$_2$ in a molar ratio of 3:2:1 at 720 °C for 6 days (see the Supporting Information). IR data (KBr, cm^{-1}): 990 (vw), 928 (vs), 895 (vs), 770 (s), 748 (s), 670 (vs), 652 (s), 636 (vs), 478 (m), 456 (s), 417 (w).

Single-Crystal Structure Determination. Data collections for the two compounds were performed on a Rigaku Mercury CCD diffractometer equipped with a graphite-monochromated Mo Kα radiation source (λ = 0.71073 Å) at 293 K. Both data sets were corrected for Lorentz and polarization factors as well as for absorption by the multiscan method.[9a] Both structures were solved by direct methods and refined by full-matrix least-squares fitting on F^2 by *SHELX-97*.[9b] All of the atoms were refined with anisotropic thermal parameters. Crystallographic data and structural refinements for the two compounds are summarized in Table 1. Important bond distances are listed in Table 2. More details on the crystallographic studies as well as atomic displacement parameters are given as Supporting Information.

Computational Descriptions. The crystallographic data of the two compounds were used for the band-structure calculations. The ab initio band-structure calculations were performed by using the computer code *CASTEP*.[10] This code employs density functional theory (DFT) using a plane-wave basis set with Vanderbilt ultrasoft pseudopotentials to approximate the interactions between core and valence electrons.[11] The exchange-correlation energy was calculated using the Perdew−Burke−Ernzerhof modification to the generalized gradient approximation.[12] A kinetic-energy cutoff of 300 eV was used throughout our work. Pseudoatomic calculations were performed for O $2s^22p^4$, Se $4s^24p^4$, Te $5s^25p^4$, Mo $4s^24p^64d^55s^1$, and Ni $3d^84s^2$. The parameters used in the calculations and convergence criteria were set by the default values of the *CASTEP* code.[10]

Results and Discussion

Solid-state reactions of nickel(II) oxide, molybdenum(VI) oxide, and SeO$_2$ or TeO$_2$ afforded two new nickel(II)

(9) (a) *CrystalClear,* version 1.3.5; Rigaku Corp.: Woodlands, TX, 1999. (b) Sheldrick, G. M. *SHELXTL, Crystallographic Software Package*, version 5.1; Bruker-AXS: Madison, WI, 1998.
(10) (a) Segall, M. D.; Lindan, P. L. D.; Probert, M. J.; Pickard, C. J.; Hasnip, P. J.; Clark, S. J.; Payne, M. C. *J. Phys.: Condens. Matter* **2002**, *14*, 2717. (b) Segall, M.; Lindan, P.; Probert, M.; Pickard, C.; Hasnip, P.; Clark, S.; Payne, M. *Materials Studio CASTEP*, version 2.2; Accelerys, Inc.: San Diego, CA, 2002.
(11) Vanderbilt, D. *Phys. Rev. B: Condens. Matter Mater. Phys.* **1990**, *41*, 7892.
(12) Perdew, J. P.; Burke, K.; Ernzerhof, M. *Phys. Rev. Lett.* **1996**, *77*, 3865.

Table 2. Important Bond Lengths (Å) and Bond Angles (deg) for Ni₃(Mo₂O₈)(XO₃) (X = Se, Te)[a]

Ni₃(Mo₂O₈)(SeO₃)			
Ni(1)−O(11)	1.988(4)	Ni(1)−O(9)#1	2.081(4)
Ni(1)−O(9)#2	2.082(5)	Ni(1)−O(3)	2.090(4)
Ni(1)−O(8)	2.108(5)	Ni(1)−O(2)	2.132(5)
Ni(2)−O(10)#3	1.983(4)	Ni(2)−O(3)#2	2.014(5)
Ni(2)−O(1)	2.039(4)	Ni(2)−O(7)#4	2.084(5)
Ni(2)−O(9)	2.091(4)	Ni(2)−O(2)#5	2.160(4)
Ni(3)−O(5)#6	2.013(4)	Ni(3)−O(4)	2.016(4)
Ni(3)−O(6)	2.021(5)	Ni(3)−O(2)#4	2.042(5)
Ni(3)−O(8)#4	2.084(4)	Ni(3)−O(7)#5	2.091(4)
Mo(1)−O(4)	1.721(4)	Mo(1)−O(5)	1.722(4)
Mo(1)−O(8)	1.914(4)	Mo(1)−O(7)	1.926(5)
Mo(1)−O(6)#4	2.271(4)	Mo(1)−O(6)#1	2.283(4)
Mo(2)−O(11)	1.719(4)	Mo(2)−O(10)	1.723(4)
Mo(2)−O(9)	1.893(4)	Mo(2)−O(6)	1.965(4)
Mo(2)−O(7)#4	2.284(5)	Mo(2)−O(8)#5	2.304(4)
Se(1)−O(1)	1.659(5)	Se(1)−O(3)#3	1.708(4)
Se(1)−O(2)	1.780(5)		
O(8)−Mo(1)−O(7)	148.0(2)	O(5)−Mo(1)−O(6)#4	162.8(2)
O(4)−Mo(1)−O(6)#1	163.5(2)	O(9)−Mo(2)−O(6)	145.6(2)
O(10)−Mo(2)−O(7)#4	161.8(2)	O(11)−Mo(2)−O(8)#5	163.9(2)
Ni₃(Mo₂O₈)(TeO₃)			
Ni(1)−O(7)#1	2.021(2)	Ni(1)−O(2)#2	2.027(2)
Ni(1)−O(6)#3	2.045(2)	Ni(1)−O(2)#4	2.052(2)
Ni(1)−O(1)	2.087(2)	Ni(1)−O(3)#5	2.142(2)
Ni(2)−O(5)#6	2.011(2)	Ni(2)−O(5)	2.011(2)
Ni(2)−O(4)#5	2.015(3)	Ni(2)−O(1)	2.064(3)
Ni(2)−O(3)#5	2.099(2)	Ni(2)−O(3)#7	2.099(2)
Mo(1)−O(5)#8	1.737(2)	Mo(1)−O(5)	1.737(2)
Mo(1)−O(3)	1.911(2)	Mo(1)−O(3)#8	1.911(2)
Mo(1)−O(4)	2.274(2)	Mo(1)−O(4)#9	2.274(2)
Mo(2)−O(7)	1.732(2)	Mo(2)−O(7)#1	1.732(2)
Mo(2)−O(6)	1.812(3)	Mo(2)−O(4)	1.980(3)
Mo(2)−O(3)#8	2.319(2)	Mo(2)−O(3)#9	2.319(2)
Te(1)−O(2)#6	1.863(2)	Te(1)−O(2)	1.863(2)
Te(1)−O(1)	1.923(3)		
O(3)−Mo(1)−O(3)#8	149.1(1)	O(5)#8−Mo(1)−O(4)	163.4(1)
O(5)−Mo(1)−O(4)#9	163.4(1)	O(6)−Mo(2)−O(4)	143.6(1)
O(7)−Mo(2)−O(3)#8	162.8(1)	O(7)#1−Mo(2)−O(3)#9	162.8(1)

[a] Symmetry transformations used to generate equivalent atoms. For Ni₃(Mo₂O₈)(SeO₃): #1, x, $y − 1$, z; #2, $−x + 1$, $−y + 1$, $−z + 2$; #3, $x + 1$, y, z; #4, $−x + 1$, $−y + 1$, $−z + 1$; #5, x, $y + 1$, z; #6, $− x$, $−y + 1$, $−z + 1$. For Ni₃(Mo₂O₈)(TeO₃): #1, x, $−y + 1/2$, z; #2, $−x + 1$, y, $−z$; #3, $x + 1/2$, $y − 1/2$, z; #4, $x + 1/2$, $−y + 1/2$, z; #5, $−x + 3/2$, $−y + 1/2$, $−z + 1$; #6, x, $−y$, z; #7, $−x + 3/2$, $y − 1/2$, $−z + 1$; #8, $−x + 1$, y, $−z + 1$; #9, $−x + 1$, $−y + 1$, $−z + 1$.

molybdenum(VI) selenite and tellurite compounds, namely, Ni₃(Mo₂O₈)(XO₃) (X = Se, Te). The syntheses of Ni₃-(Mo₂O₈)(XO₃) (X = Se, Te) can be expressed by the following reactions at 710 or 720 °C: 3NiO + 2MoO₃ + XO₂ → Ni₃(Mo₂O₈)(XO₃) (X = Se, Te). They display two different types of 3D structures containing [Mo₄O₁₆]⁸⁻ clusters and [Ni₆O₂₂]³²⁻ clusters or 1D nickel oxide chains. These two compounds represent the first examples of nickel-(II) selenite and tellurite decorated by polyoxomolybdate clusters.

The structure of Ni₃(Mo₂O₈)(SeO₃) features a 3D network in which [Ni₆O₂₂]³²⁻ cluster units are interconnected by [Mo₄O₁₆]⁸⁻ clusters and SeO₃²⁻ anions (Figure 1). All three Ni(II) ions in the asymmetric unit are octahedrally coordinated by six oxygen atoms with Ni−O distances ranging from 1.983(4) to 2.160(4) Å (Table 2), which are comparable to those reported in other nickel(II) selenites.[13] Both Mo atoms are octahedrally coordinated by six oxygen atoms. The Mo−O bond distances are in the range of 1.721(4)−2.283(4)
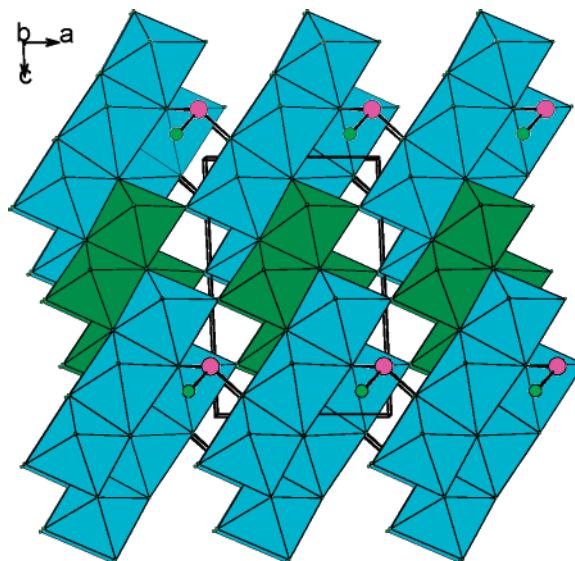
Figure 1. View of the structure of Ni₃(Mo₂O₈)(SeO₃) down the *b* axis. The NiO₆ and MoO₆ octahedra are shaded in cyan and olive, respectively. Se and O atoms are drawn as pink and green circles, respectively.

and 1.719(4)−2.304(4) Å, respectively, for Mo(1) and Mo(2) atoms (Table 2). Hence, both MoO₆ octahedra are severely distorted. The Mo(1) atom is distorted toward an edge (O(4)⋯O(5) (local C_2 direction) with two "short" (1.721(4) and 1.722(4) Å), two "normal" (1.914(4) and 1.926(5) Å), and two "long" (2.271(4) and 2.283(4) Å) Mo⁶⁺−O bonds (Figure 2a, Table 2).[3d] The Mo(2) atom adopts a similar distortion to that of Mo(1) (Figure 2a, Table 2). Taking into account the six Mo−O bond lengths as well as the deviations of the three trans O−Mo−O bond angles from 180°, the magnitudes of the distortions (Δ_d) were calculated to be 1.18 and 1.29 Å, respectively for Mo(1) and Mo(2), both of which are very strong ($\Delta_d > 0.8$ Å).[3d] The Se^{IV} atom is in a ψ-SeO₃ trigonal-pyramidal geometry with the lone pair of Se^{IV} occupying the pyramidal site. The Se−O distances range from 1.659(5) to 1.780(5) Å (Table 2). Bond-valence calculations indicate that the Ni atom is in an oxidation state of +2 and that the Mo and Se atoms are in the states of +6 and +4, respectively. The calculated total bond valences for the Ni(1), Ni(2), Ni(3), Mo(1), Mo(2), and Se(1) atoms are 1.91, 2.02, 2.10, 5.97, 5.90, and 3.92, respectively.[14]

The four Mo^{VI}O₆ octahedra are interconnected by edge-sharing (O(6)⋯O(7) and O(6)⋯O(8)) bonds to form a cyclic [Mo₄O₁₆]⁸⁻ tetranuclear cluster unit. The Mo⋯Mo separations for a pair of edge-sharing MoO₆ octahedra are in the range of 3.297(1)−3.722(1) Å. O(6) is a μ_3 metal linker and bridges with three Mo^{VI} centers (2 Mo1 and 1 Mo2). It should be noted that such cyclic Mo₄ clusters have been observed in many molybdenum(VI) coordination compounds.[15]

(13) (a) Johnsson, M.; Törnroos, K. W.; Lemmens, P.; Millet, P. *Chem. Mater.* **2003**, *15*, 68. (b) Shen, Y. L.; Mao, J.-G.; Jiang, H. L. *J. Solid State Chem.* **2005**, *178*, 2949. (c) Johnsson, M.; Lidin, S.; Törnroos, K. W.; Bürgi, H. B.; Millet, P. *Angew. Chem., Int. Ed.* **2004**, *43*, 4292. (d) Jiang, H. L.; Mao, J. G. *Inorg. Chem.* **2006**, *45*, 7593.
(14) (a) Brown, I. D.; Altermatt, D. *Acta Crystallogr.* **1985**, *B41*, 244. (b) Brese, N. E.; O'Keeffe, M. *Acta Crystallogr.* **1991**, *B47*, 192.
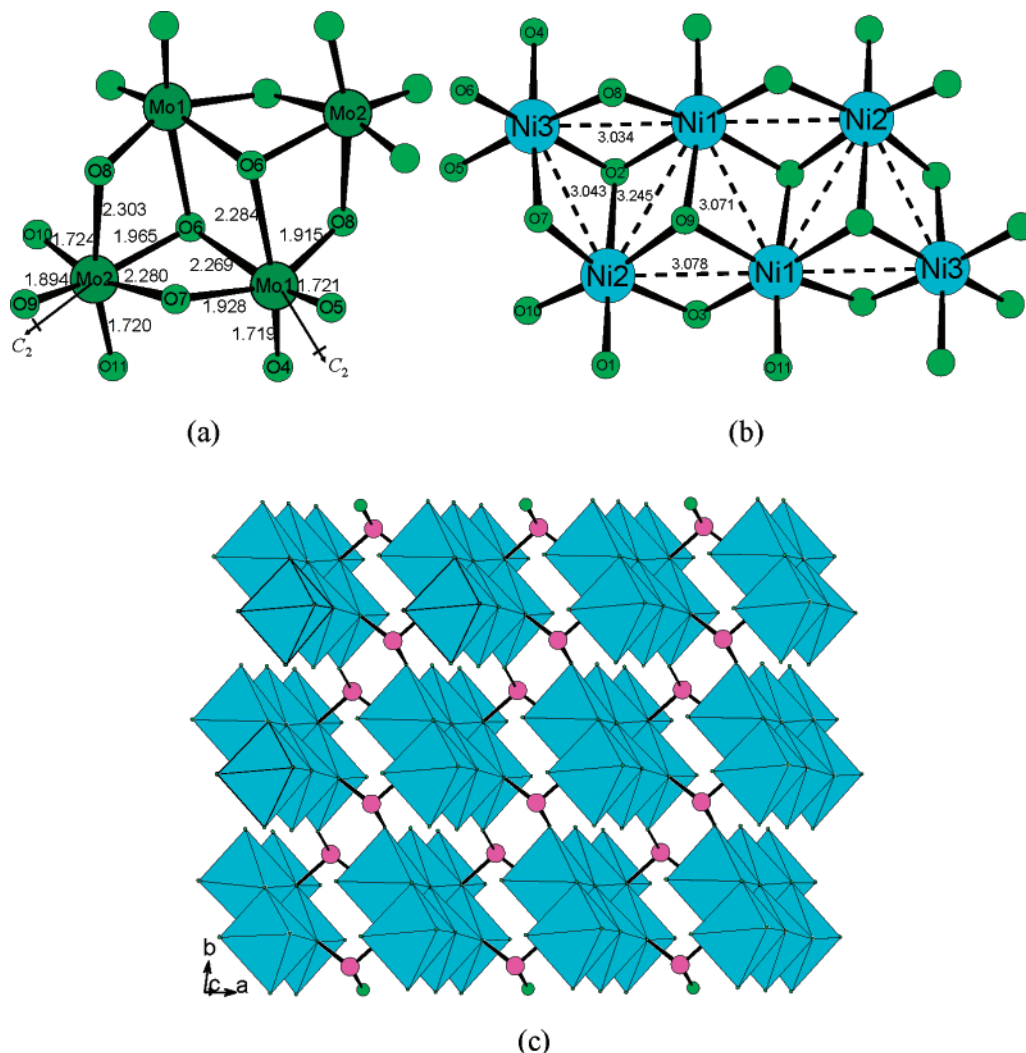
(a)

(b)

(c)

Figure 2. (a) A $[Mo_4O_{16}]^{8-}$ tetranuclear cluster unit in $Ni_3(Mo_2O_8)(SeO_3)$. (b) A $[Ni_6O_{22}]^{32-}$ hexanuclear cluster unit in $Ni_3(Mo_2O_8)(SeO_3)$. (c) A nickel(II) selenium(IV) oxide layer in $Ni_3(Mo_2O_8)(SeO_3)$.

Six NiO_6 octahedra are interconnected into a hexanuclear $[Ni_6O_{22}]^{32-}$ cluster unit through edge-sharing bonds ($O(2)\cdots$ $O(7)$, $O(2)\cdots O(8)$, $O(2)\cdots O(9)$ and $O(3)\cdots O(9)$). Both $O(2)$ and $O(9)$ act as μ_3 metal linkers (Figure 2b). The intracluster $Ni\cdots Ni$ separations between a pair of edge-sharing NiO_6 octahedra are in the range of 3.034(1)−3.245(1) Å (Figure 2b). To the best of our knowledge, this type of Ni_6 cluster has not been reported.

The $[Ni_6O_{22}]^{32-}$ cluster units are bridged by SeO_3^{2-} groups to form a 2D nickel selenite layer parallel to the *ab* plane (Figure 2c). Each SeO_3^{2-} anion is bridged to three clusters by its three oxygen atoms. $O(1)$ is monodentate and connects with a nickel(II) ion of a cluster unit, $O(2)$ connects with two nickel(II) ions from another cluster unit, and $O(3)$ is bridged to three nickel(II) ions from the third cluster (Figure 2c). Neighboring nickel selenite layers are further interconnected by the $[Mo_4O_{16}]^{8-}$ clusters via Mo−O−Ni bridges

into a 3D network structure. The lone-pair electrons of the selenium(IV) atoms are orientated to the cavities of the structure (Figure 1).

The structure of $Ni_3(Mo_2O_8)(TeO_3)$ features a 3D structure in which the corrugated nickel oxide anionic chains are bridged by $[Mo_4O_{16}]^{8-}$ cluster units and TeO_3^{2-} anions (Figure 3). There are two unique Ni atoms, two Mo atoms, and one Te atom in the asymmetric unit. All the Ni and Mo atoms are octahedrally coordinated by six oxygens. The Ni−O distances range from 2.011(2) to 2.142(2) Å (Table 2), which are comparable to those in $Ni_3(Mo_2O_8)(SeO_3)$ and other nickel(II) tellurites reported.[13] Similar to that in Ni_3-$(Mo_2O_8)(SeO_3)$, the Mo^{VI} atoms are in a severely distorted octahedral-coordinated environment with Mo−O bond lengths ranging from 1.732(2) to 2.319(2) Å (Table 2). Likewise, in $Ni_3(Mo_2O_8)(SeO_3)$, the $Mo(1)O_6$ octahedron in $Ni_3(Mo_2O_8)$-(TeO_3) is distorted toward an edge ($O(5)\cdots O(5)$) (local C_2 direction distortion) (Figure 4a, Table 2).[3d] The $Mo(2)O_6$ octahedron is also distorted toward an edge ($O(7)\cdots O(7)$) (Figure 4a, Table 2). The magnitudes of the distortion (Δ_d) were calculated to be 1.12 and 1.44 Å, respectively, for Mo(1) and Mo(2),[3d] which are very strong and comparable

(15) (a) Chisholm, M. H.; Huffman, J. C.; Kirkpatrick, C. C.; Leonelli, J.; Folting, K. *J. Am. Chem. Soc.* **1981**, *103*, 6093. (b) Liu, S. C.; Shaikh, S. N.; Zubieta, J. *Inorg. Chem.* **1987**, *26*, 4303. (c) Kang, H.; Liu, S. C.; Shaikh, S. N.; Nicholson, T.; Zubieta, J. *Inorg. Chem.* **1989**, *28*, 920. (d) Limberg, C.; Buchner, M.; Heinze, K.; Walter, O. *Inorg. Chem.* **1997**, *36*, 872.
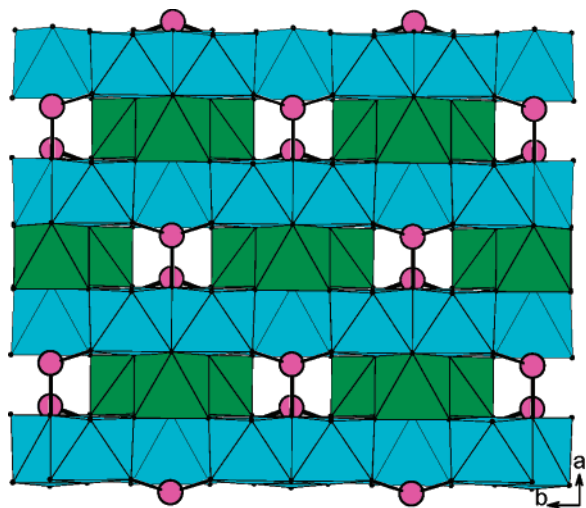
Figure 3. View of the structure of $Ni_3(Mo_2O_8)(TeO_3)$ down the *c* axis. The NiO_6 and MoO_6 octahedra are shaded in cyan and olive, respectively. Te atoms are drawn as pink circles.

to those of $Ni_3(Mo_2O_8)(SeO_3)$. The Te^{IV} atom is coordinated by three oxygen atoms in a distorted ψ-TeO_3 tetrahedral geometry, with the fourth site occupied by the lone-pair electrons with Te−O distances ranging from 1.863(2) to 1.923(3) Å. The oxidation states of the Ni, Mo, and Te atoms are +2, +6, and +4, respectively, according to the results of bond-valence calculations.[14] The calculated total bond valences for the Ni(1), Ni(2), Mo(1), Mo(2), and Te(1) atoms are 2.00, 2.07, 5.89, 5.98, and 3.88, respectively.

Similar to that in $Ni_3(Mo_2O_8)(SeO_3)$, the four $Mo^{VI}O_6$ octahedra in $Ni_3(Mo_2O_8)(TeO_3)$ are interconnected via edge-sharing to form a $[Mo_4O_{16}]^{8-}$ tetranuclear cluster unit (Figure 4a).

Two $Ni(1)O_6$ and one $Ni(2)O_6$ octahedra are interconnected via edge-sharing (O(1)···O(3) and O(1)···O(6)) into a $[Ni_3O_{13}]^{20-}$ trinuclear unit. Neighbors of such trinuclear units are further interconnected through edge-sharing (O(2)···O(2)) into a corrugated $[Ni_3O_{11}]^{16-}$ anionic chain along the *b* axis with the Ni(1)−O(2)−Ni(1) bond angle of 84.65(9)° (Figure 4b). The intercluster Ni···Ni separation is 3.016(2) Å, whereas the intracluster Ni(1)···Ni(1) and Ni(1)···Ni(2) distances are 3.072(1) and 3.021(1) Å, respectively. This nickel oxide chain can also be viewed as $Ni(2)O_6$ octahedra being grafted onto the corrugated chain of $Ni(1)O_6$ through edge-sharing (O(3)···O(1) and O(2)···O(2)). Such a corrugated nickel(II) oxide chain has not been reported, and only simple 1D nickel oxide single chains were characterized in $Ni(SeO_4)(H_2O)$ and $NiTe_2O_5$.[16] It is interesting to note that $[Ni_6O_{22}]^{32-}$ clusters are formed in $Ni_3(Mo_2O_8)(SeO_3)$, whereas corrugated $[Ni_3O_{11}]^{16-}$ anionic chains are observed in $Ni_3(Mo_2O_8)(TeO_3)$. Both nickel oxide building units are based on Ni_3O triangles. The Ni_3O triangles in $[Ni_6O_{22}]^{32-}$ clusters are condensed via sharing Ni−Ni edges whereas those in $[Ni_3O_{11}]^{16-}$ anionic chains are interconnected through Ni−O−Ni bridges. These different

(16) (a) Giester, G.; Wildner, M. *Neues Jahrb. Mineral. Monatsh.* **1992**, *1992*, 135. (b) Platte, C.; Troemel, M. *Acta Crystallogr.* **1981**, *B37*, 1276.

nickel(II) oxide architectures may result from the different coordination modes of the selenite and tellurite groups as well as the different ionic radii of Se^{IV} and Te^{IV}.

Neighboring corrugated nickel(II) oxide chains are bridged by TeO_3^{2-} anions to form a thick nickel(II) tellurite layer parallel to the *ab* plane. Different from the SeO_3^{2-} group in $Ni_3(Mo_2O_8)(SeO_3)$, each TeO_3 group bridges with seven nickel(II) ions: O(1) connects with three nickel(II) ions from one nickel(II) oxide chain whereas two O(2) atoms bridge with four nickel(II) ions from another nickel(II) oxide chain. The thickness of the layer is about 12.1 Å. Such layers are further interconnected by the $[Mo_4O_{16}]^{8-}$ clusters via Mo−O−Ni bridges into a 3D network structure. The lone-pair electrons of the tellurium(IV) atoms are orientated to the tunnels of the structure (Figure 3). The effective volume of the lone-pair electrons is approximately the same as the volume of an O^{2-} anion, according to Galy et al.[17]

Magnetic Properties. $Ni_3(Mo_2O_8)(SeO_3)$ obeys the Curie−Weiss law in the temperature range of 50−300 K; below 50 K, a slight deviation was observed (Figure 5a). At 300 K, the $\chi_M T$ value is 3.99 emu·mol^{-1}·K, which corresponds to an effective magnetic moment (μ_{eff}) of 5.65 μ_B for three isolated Ni^{2+} ($S = 1$, $g = 2.4957$) ions. The $\chi_M T$ value increases upon cooling and reaches a maximum of 5.52 emu·mol^{-1}·K at 28 K. Below 28 K, it decreases continuously upon cooling and a value of 0.51 emu·mol^{-1}·K is reached at 2.0 K. The linear fit of the magnetic data in the range of 50−300 K gave a Weiss constant (θ) of 15.4(2) K, indicating significant ferromagnetic interactions between magnetic centers. It is expected that the magnetic interactions should be dominated by the magnetic interactions between nickel(II) ions within the hexanuclear $[Ni_6O_{22}]^{32-}$ cluster. As mentioned before, the intracluster Ni···Ni separations are in the range of 3.034(1)−3.245(1) Å. The shortest intercluster Ni···Ni contact is 4.666(1) Å. $Ni_3(Mo_2O_8)(TeO_3)$ obeys the Curie−Weiss law in the temperature range of 50−300 K; below about 50 K, a significant deviation was observed (Figure 5b). At 300 K, the $\chi_M T$ value is 3.92 emu·mol^{-1}·K, which corresponds to an effective magnetic moment (μ_{eff}) of 5.62 μ_B for three isolated Ni^{2+} ($S = 1$, $g = 2.28$) ions. The $\chi_M T$ value increases upon cooling and reaches a maximum of at 4.28 emu·mol^{-1}·K at 56 K. Below 56 K, it decreases continuously upon cooling and a value of 0.32 emu·mol^{-1}·K is reached at 2.0 K. The linear fit of the magnetic data in the range of 50−300 K gave a Weiss constant (θ) of 5.5(1) K, indicating weak ferromagnetic interactions between Ni^{2+} ions. It is expected that such magnetic interactions are dominated by the magnetic interactions between the Ni(II) ions within the 1D $[Ni_3O_{11}]^{16-}$ anionic chain. As mentioned earlier, the Ni···Ni separations between pairs of edge-sharing NiO_6 octahedra are in the range of 3.016(2)−3.072(1) Å. The shortest interchain Ni···Ni separation is 4.715(1) Å.

Thermogravimetric Analysis. TGA analyses under an air atmosphere indicate that $Ni_3(Mo_2O_8)(SeO_3)$ and $Ni_3(Mo_2O_8)(TeO_3)$ are stable up to 570 and 850 °C, respectively (Figure

(17) Galy, J.; Meunier, G.; Andersson, S.; Åström, A. *J. Solid State Chem.* **1975**, *13*, 142.
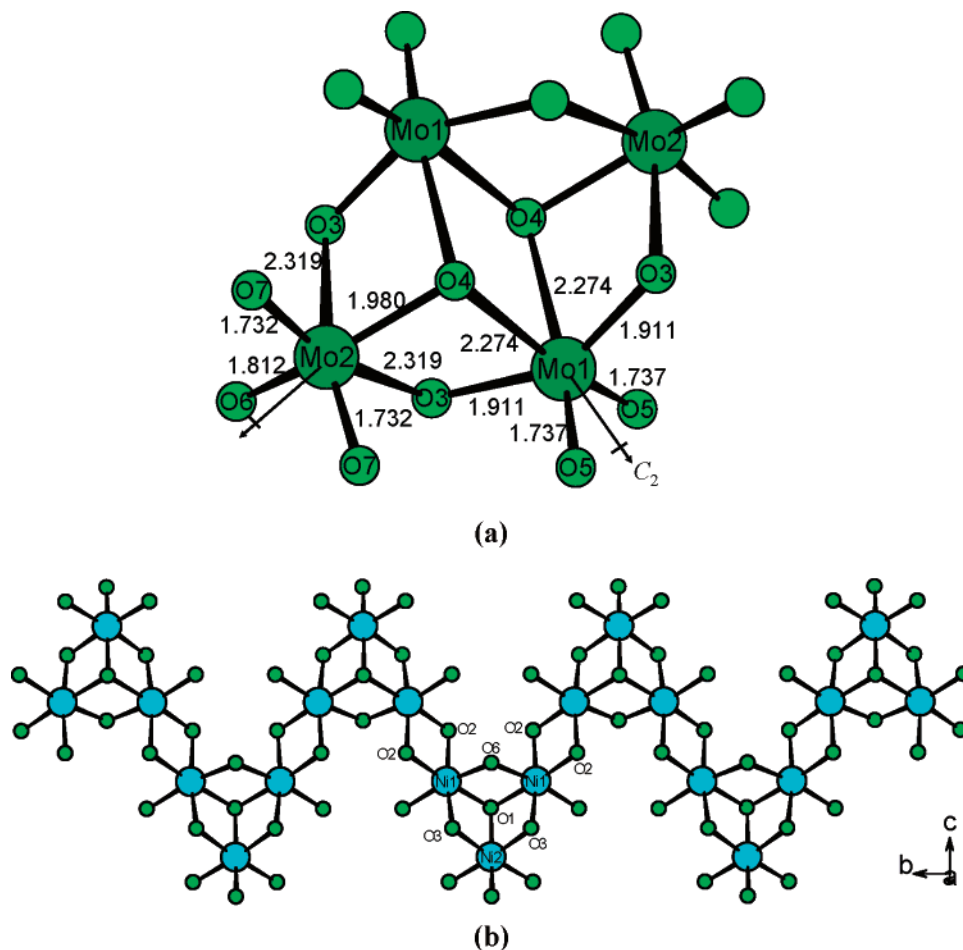
Figure 4. (a) A [Mo$_2$O$_{14}$]$^{16-}$ cluster unit in Ni$_3$(Mo$_2$O$_8$)(TeO$_3$). (b) A 1D [Ni$_3$O$_{11}$]$^{16-}$ corrugated chain along the *b* axis in Ni$_3$(Mo$_2$O$_8$)(TeO$_3$).

6). Both compounds exhibit two main steps of weight loss. The first steps of weight loss occurred in the temperature ranges of 570−895 and 850−1100 °C, respectively, for Ni$_3$(Mo$_2$O$_8$)(SeO$_3$) and Ni$_3$(Mo$_2$O$_8$)(TeO$_3$), which corresponds to the release of 1 mol of SeO$_2$ or TeO$_2$ per formula unit. The observed weight losses of 17.8% for Ni$_3$(Mo$_2$O$_8$)-(SeO$_3$) and 22.3% for Ni$_3$(Mo$_2$O$_8$)(TeO$_3$) are close to the calculated ones (17.8 and 23.8%, respectively). Ni$_3$(Mo$_2$O$_8$)-(SeO$_3$) exhibits a plateau in the wide range of 895−1100 °C. Above 1100 °C, both compounds are further decomposed. The total weight losses at 1300 °C are 36.0 and 31.0%, respectively, for the Se and Te compounds, and the final residuals are not characterized due to the fact that the residuals had been melted by the TGA buckets (made of Al$_2$O$_3$) under such high temperatures.

Band Structure and Density of States. Spin-polarized band-structure calculations for Ni$_3$(Mo$_2$O$_8$)(XO$_3$) (X = Se, Te) based on the DFT method have been made. On the basis of the calculations, the integrated spin density (12.0 e) and integrated absolute spin density (12.5628 and 12.4764 e, respectively, for Se and Te compounds) per unit cell are almost identical, indicating possible ferromagnetic interactions between nickel(II) centers in both compounds, which is in good agreement with the results from magnetic measurements.

The band structures of both compounds are similar and display a small band gap (see the Supporting Information).

The top of the valence bands (VBs) is nearly flat and close to the Fermi level (0.0 eV), and the bottom of the conduction bands (CBs) exhibits small dispersion. For Ni$_3$(Mo$_2$O$_8$)-(SeO$_3$), both the lowest energy (0.75 eV) of the CBs and the highest energy (−0.01 eV) of the VBs are located at the G point (Table 3). Hence, it represents a semiconductor character with a direct band gap of around 0.76 eV. As for Ni$_3$(Mo$_2$O$_8$)(TeO$_3$), the lowest of the CBs with energy of 0.76 eV is located at the M point, and the highest of the VBs is located at the V point with an energy of 0.00 eV (Table 3). Therefore, it is reasonable to consider Ni$_3$(Mo$_2$O$_8$)-(TeO$_3$) as a semiconductor with an indirect band gap of 0.76 eV. The absorption edges of both compounds are very close to 1715 nm (0.72 eV), and both compounds exhibit strong absorption peaks at 360 nm (3.45 eV), 770 nm (1.61 eV), and 1270 nm (0.98 eV) (See the Supporting Information). Hence, our calculated band gaps are close to those of the experimental results.

For both compounds, the VBs lying near −62.6 and −36.9 eV are mainly the contributions of the Mo 4s and Mo 4p states, respectively (see the Supporting Information). The O 2s and Se 4s (or Te 5s) states dominate the VBs between −22.2 and −10.0 eV. The main contributions of the VBs, ranging from −7.9 eV to the Fermi level, are the Ni 3d and O 2p states, with a small mixing of Mo 4d and Se 4p (or Te 5p) states. The CBs are dominated by unoccupied Ni 3d, Mo 4d, and O 2p states. The Ni 3d states are found to be
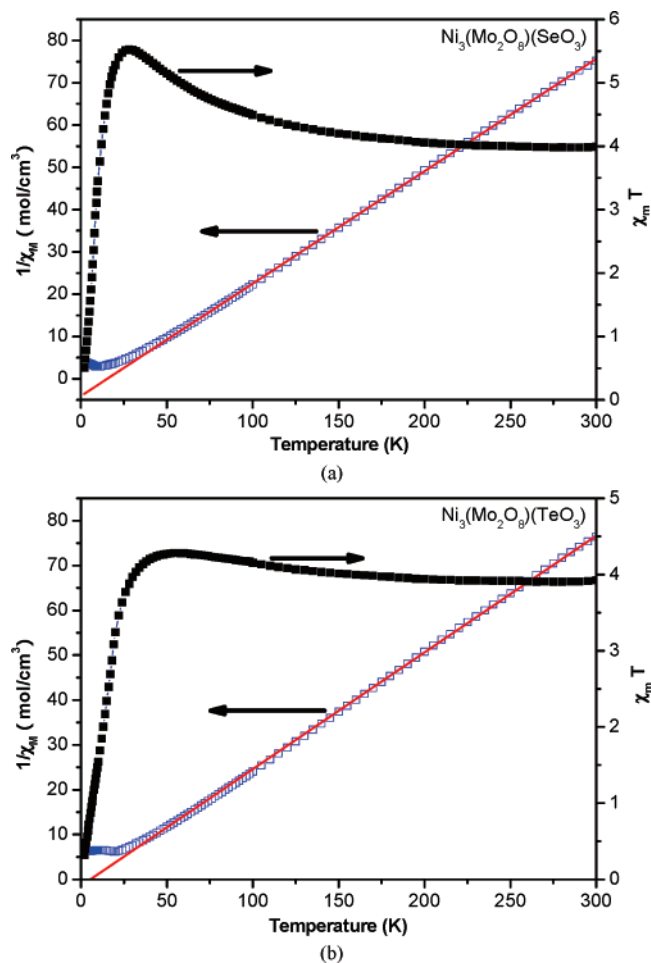
Figure 5. χ versus T and χT versus T plots for $Ni_3(Mo_2O_8)(SeO_3)$ (a) and $Ni_3(Mo_2O_8)(TeO_3)$ (b). The red line represents the linear fit of data according to the Curie−Weiss law.

spin-polarized, which is responsible for the ferromagnetism of the two compounds. It is observed that the Ni 3d states display two peaks, which correspond to the doubly degenerate e_g states and threefold degenerate t_{2g} states of the octahedrally coordinated nickel(II) ions.

The chemical bonds for both compounds were studied by population analyses. The calculated bond orders are 0.16−0.32, 0.15−0.80, and 0.18−0.52 e for Ni−O, Mo−O, and X−O bonds, respectively (Table 4). It is generally assumed that a covalent single-bond order corresponds to 1.0 e. It is observed that the elongated Mo−O bonds are much weaker than those of the normal Mo−O bonds; the latter are also significantly weaker than those of the short Mo−O bonds (Table 4).
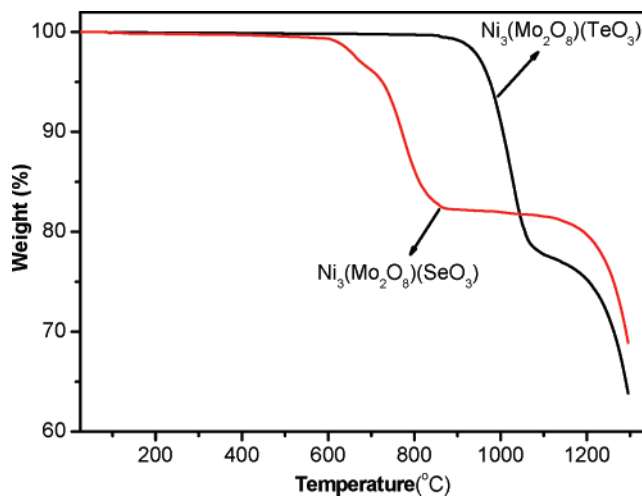

Figure 6. TGA curves for $Ni_3(Mo_2O_8)(XO_3)$ (X = Se, Te).

Table 3. The State Energies (eV) of the Lowest Conduction Band (L-CB) and the Highest Valence Band (H-VB) at Some k Points for $Ni_3(Mo_2O_8)(XO_3)$ (X = Se, Te)

	$Ni_3(Mo_2O_8)(SeO_3)$			
k point	G	F	X	Z
L-CB	0.75206	0.80638	0.85980	0.81896
H-VB	−0.00771	−0.03240	−0.04425	−0.01634

	$Ni_3(Mo_2O_8)(TeO_3)$				
k point	L	M	A	G	Z	V
L-CB	0.92117	0.76385	0.82050	0.91676	0.92117	0.90344
H−VB	−0.06470	−0.03491	−0.05261	−0.00592	−0.06470	0

Table 4. The Calculated Bond Orders of $Ni_3(Mo_2O_8)(XO_3)$ (X = Se, Te)

	$Ni_3(Mo_2O_8)(SeO_3)$		$Ni_3(Mo_2O_8)(TeO_3)$	
bond	bond length	bond order	bond length	bond order
Ni−O	1.983−2.159	0.16−0.32	2.011−2.142	0.17−0.31
Mo−O	1.719−1.724	0.78−0.79	1.732−1.737	0.80
Mo−O	1.895−1.965	0.41−0.48	1.812−1.980	0.38−0.53
Mo−O	2.269−2.303	0.15−0.16	2.274−2.319	0.15−0.17
X−O	1.661−1.780	0.18−0.52	1.864	0.18−0.37

Supporting Information Available: X-ray crystallographic files in CIF format, simulated and experimental XRD powder patterns, and diagrams for band structures and density-of-states for $Ni_3(Mo_2O_8)(SeO_3)$ and $Ni_3(Mo_2O_8)(TeO_3)$. This material is available free of charge via the Internet at http://pubs.acs.org.

IC700500Q